

Digitoxin-Induced Cytotoxicity in Cancer Cells Is Mediated through Distinct Kinase and Interferon Signaling Networks

Ioannis Prassas^{1,2}, George S. Karagiannis^{1,2}, Ihor Batruch⁴, Apostolos Dimitromanolakis^{1,2}, Alessandro Datti^{2,3,5}, and Eleftherios P. Diamandis^{1,2,4}

Abstract

Cardiac glycosides (e.g., digoxin, digitoxin) constitute a diverse family of plant-derived sodium pump inhibitors that have been in clinical use for the treatment of heart-related diseases (congestive heart failure, atrial arrhythmia) for many years. Recently though, accumulating *in vitro* and *in vivo* evidence highlight potential anticancer properties of these compounds. Despite the fact that members of this family have advanced to clinical trial testing in cancer therapeutics, their cytotoxic mechanism is not yet elucidated. In this study, we investigated the cytotoxic properties of cardiac glycosides against a panel of pancreatic cancer cell lines, explored their apoptotic mechanism, and characterized the kinetics of cell death induced by these drugs. Furthermore, we deployed a high-throughput kinome screening approach and identified several kinases of the Na-K-ATPase-mediated signal transduction circuitry (epidermal growth factor receptor, Src, pKc, and mitogen-activated protein kinases) as important mediators downstream of cardiac glycoside cytotoxic action. To further extend our knowledge on their mode of action, we used mass-spectrometry-based quantitative proteomics (stable isotope labeling of amino acids in cell culture) coupled with bioinformatics to capture large-scale protein perturbations induced by a physiological dose of digitoxin in BxPC-3 pancreatic cancer cells and identified members of the interferon family as key regulators of the main protein/protein interactions downstream of digitoxin action. Hence, our findings provide more in-depth information regarding the molecular mechanisms underlying cardiac glycoside-induced cytotoxicity. *Mol Cancer Ther*; 10(11); 2083–93. ©2011 AACR.

Introduction

Cardiac glycosides constitute a diverse family of naturally derived compounds, widely known for their ability to bind to, and inhibit, the sodium pump. For many years, members of this family (digoxin, digitoxin) have been in clinical use for the treatment of heart failure and atrial arrhythmia (1). However, some early epidemiologic studies, describing significantly lower growth potential of tumors on patients on digitalis treatment, sparked new interest in the anticancer properties of these drugs (2).

Numerous subsequent *in vitro* studies revealed an increased susceptibility of cancer cells to the effects of these compounds. It is now well shown that low doses of cardiac glycosides may activate downstream proapoptotic pathways in several cancer cell lines, without any profound effect in normal cells (3, 4). A plethora of mechanisms has been recently proposed to account for this preferential cytotoxicity in cancer cells, including inhibition of glycolysis, cancer-specific overexpression of sodium pump subunits and inhibition of N-glycan expression (5–7). Moreover, the successful outcomes of recent *in vivo* studies have channeled several members of this family into clinical trials for cancer therapies (8).

At the mechanistic level, many different pathways have been suggested to be associated with the cytotoxic action of these drugs including calcium-dependent activation of caspases and other hydrolytic enzymes, generation of reactive oxygen species (ROS), topoisomerase inhibition, interference with signal transduction pathways, induction of the cell-cycle inhibitor p21^{Cip1} and inhibition of hypoxia-inducible factor1a synthesis (1). Consequently, these compounds may produce a broad spectrum of cellular responses eventually leading to cell death.

In this study, we attempted to provide a better insight into the cardiac glycoside cytotoxic mode of action. To

Authors' Affiliations: ¹Department of Laboratory Medicine and Pathobiology, University of Toronto; ²Samuel Lunenfeld Research Institute and Department of Pathology and Laboratory Medicine, Mount Sinai Hospital; ³Sinai-McLaughlin Assay and Robotic Technologies Facility, Samuel Lunenfeld Research Institute; ⁴Department of Clinical Biochemistry, University Health Network, Toronto, Ontario, Canada; and ⁵Department of Experimental Medicine and Biochemical Sciences, University of Perugia, Perugia, Italy

Note: Supplementary data for this article are available at Molecular Cancer Therapeutics Online (<http://mct.aacrjournals.org/>).

Corresponding Author: Eleftherios P. Diamandis, Mount Sinai Hospital, Department of Pathology & Laboratory Medicine, ACDC Laboratory, Room L6-201, 60 Murray St., Toronto, ON, M5T 3L9 Canada. Phone: 416-586-8443; Fax: 416-619-5521; E-mail: ediamandis@mtsinai.on.ca

doi: 10.1158/1535-7163.MCT-11-0421

©2011 American Association for Cancer Research.

achieve this, we deployed a systems biology approach by integrating *in vitro* functional assays, targeted high-throughput approaches (kinome-screen), mass-spectrometry-based quantitative proteomics [stable isotope labeling of amino acids in cell culture (SILAC)], and bioinformatics (pathway analyses). As a model, we opted to focus our investigations on the effects of cardiac glycosides against a panel of pancreatic cancer cell lines, because pancreatic cancer represents the most lethal and one of the most difficult cancer type to treat with existing chemotherapeutic treatments. Our findings verify previous reports that cardiac glycosides induce apoptosis in cancer cells and additionally provide more in-depth information regarding the pathways and the key mediators downstream of cardiac glycoside action.

Materials and Methods

Cell lines

The pancreatic cancer cell lines MiaPaCa-2, BxPC-3, Panc-1, Capan-1, Su.86.86, and CFPAC-1, were obtained from the American Type Culture Collection and were cultured in their recommended media. All experiments were conducted with mycoplasma-free cell lines, all within the first 5 passages from the initiation of their cultures.

Drugs and chemical library

The targeted kinome library was provided by the Ontario Institute for Cancer Research through the Samuel Lunenfeld Research Institute's High Throughput Screening Robotics Facility, Mount Sinai Hospital, Toronto, ON, Canada. The cardiac glycosides bufalin, convallatoxin, cymarin, dixitoxigenin, digitoxin, digoxin, ouabain, peruvoside, and proscillaridin were all obtained from Sigma Chemical Co. Gemcitabine hydrochloride was purchased from Sigma-Aldrich. The Alamar Blue reagent was purchased from Invitrogen. Annexin V-fluorescein isothiocyanate and the binding buffer were purchased from Immunotech (Coulter). The benzyloxycarbonyl-Val-Ala-Asp(OMe)-fluoromethylketone(Z-VAD-FMK) pancaspase peptide inhibitor was purchased by Tocris Bioscience. RapiGest (a surfactant reagent used to enhance enzymatic digestion of proteins) was obtained from Waters Inc.

Cell viability assays

Lactate dehydrogenase cytotoxicity assay. Measurement of lactate dehydrogenase in the conditioned media of drug-treated cells was done as previously described (9).

Metabolic activity assay (Alamar Blue assay). Alamar blue is a stable, soluble, and nontoxic agent that monitors the innate metabolic activity of the cells, rendering it suitable for cell viability assessment. It consists of an oxidation-reduction indicator that yields a colorimetric change and a fluorescent signal in response to a metabolic activity. Cell lines were cultured at 37°C, 5%

CO₂ in their recommended medium supplemented with 10% FBS and 1% penicillin/streptomycin. First, cells were optimized for different parameters including, cell density, culture media selection, and duration of the assay, to minimize cell death. Cells were then trypsinized and transferred into 96-well plates (50,000 cells/well in a final volume of 200 µL/well) for 16 hours at 37°C and 95% humidity to allow for adherence. In a fully automated fashion, 10 different doses of cardiac glycosides, ranging from 1 µmol/L to 0.5 nmol/L [in 0.5% dimethyl sulfoxide (DMSO)], were dispensed to the wells and 48 hours later cells were washed twice with PBS before the addition of Alamar Blue solution (10% v/v in PBS). After 4-hour incubation, fluorescence was measured with a fluorescence spectrophotometer using 560EX nm/590EM nm filter setting and half-maximum inhibition of cell viability (IC₅₀) values were calculated for all tested cardiac glycosides.

Cell apoptosis assay (Annexin-V flow cytometric analysis). One of the most established hallmarks of apoptosis is exposure of phosphatidyl-serine to the cell surface. For the measurement of phosphatidyl-serine exposure, the Annexin-V-FITC method was used. Briefly, cells were cultured in 6-well plates (10⁶ cells/well) to 75% confluency and treated with increasing doses of cardiac glycosides. Cells were shortly trypsinized and resuspended in Annexin buffer (0.1 M HEPES, pH 7.4; 1.4 M NaCl; 25 mmol/L CaCl₂). FITC-conjugated Annexin (20 µg/mL) was added to the cells and tubes were incubated for 10 minutes in the dark. After addition of an equal volume of cold-binding buffer, flow cytometric analysis was done in the FACS Calibur flow cytometry system (Becton-Dickinson). As an extra validation, the benzyloxycarbonyl-Val-Ala-Asp(OMe)-fluoromethylketone (Z-VAD-FMK) pan-caspase peptide inhibitor was used to check whether caspases exhibit a major role in cardiac glycoside-induced apoptosis.

Real-time monitoring of cell adhesion assay (xCelligence assay). Detachment of adhering cells is another hallmark of cell death. To quantitatively monitor the viability status of cancer cells upon treatment with different doses of cardiac glycosides, we used the Real-Time Cell Analyzer Single Plate (RTCA SP) under the xCelligence name (Roche Applied Science and ACEA Biosciences), as previously described (10, 11). Briefly, BxPC3, Mia-Paca2 and Panc1 pancreatic cancer cells were seeded in their optimal densities in the wells of special 96-well tissue culture plates (E-Plate96) covered with electrodes and gold sensor arrays and were treated with 10 different doses of digitoxin, digoxin, peruvoside, and gemcitabine (the established chemotherapy for pancreatic cancer). During the assay, a (nontoxic) 20 mV voltage was applied to the electrodes and kinetic monitoring of cell death was based on real-time measurements (1 value every 2 minutes) of electrical impedance across the interdigitated micro-electrodes. The impedance measured in each well correlated with the number of attached (viable) cells to it (attached cell act as insulators of electric current). The

RTCA software statistic analysis was used to generate dose- and time-dependent logIC₅₀ values for all tested cardiac glycosides according to the manufacturer's instructions (10).

Kinome high-throughput screening assays. BxPC3 pancreatic cancer cells were seeded to 384-well culture plates at a density of 4,000 cells/well and were treated in duplicates first, with the kinome library alone and second, with the kinome library followed by digitoxin treatment (500 nmol/L). In both cases, kinase inhibitors were added 12 hours before digitoxin (or DMSO) treatment. Cell viability values were obtained 48-hour post digitoxin (or DMSO) treatment. As "rescuing" kinase inhibitors, we considered all those inhibitors the presence of which resulted in a significant decrease in the cytotoxic potency of digitoxin. In particular, we arbitrarily picked a threshold of 50% cell viability and looked for kinase inhibitors, that in duplicate measurements prevented more than half of cells from dying upon treatment with an IC₉₀ (500 nmol/L) dose of digitoxin. Data capture, storage, and analysis were done by a biostatistician. Quality and robustness of the synergistic screens was evaluated using biochemical checkpoints such as dynamic range, variability, and 'hit' rate, whose scores were incorporated in the Z factor, a well-established statistical parameter routinely used in high-throughput screening programs (12).

SILAC analysis

Metabolic labeling and experimental setup. BxPC3 cells were seeded at low confluency (~25%) in 2 T25 flasks and the cells in each flask were metabolically labeled with either heavy {Arg(+6), Lys(+8)} or light SILAC conditioned media (Dulbecco's Modified Eagle's Medium 10% dialyzed FBS), as previously described (13). Labeled BxPC3 cells were then detached (using a non-enzymatic cell dissociation buffer) and placed in new T25 flasks, in duplicates. Cells were left overnight to adhere and proliferate and were washed twice with PBS before treated with either 30 nmol/L digitoxin (heavy-labeled flasks) or DMSO (light-labeled flasks), for 48 hours. After the termination of the experiment, cells were washed twice with PBS, centrifuged at 1,500 g for 5 minutes and supernatants were discarded. Cell pellets were kept at -80°C, until further processed.

Sample preparation. For cell lysis, pellets were resuspended using 300 µL of 0.1% RapiGest (Waters Inc.) in 25 mmol/L ammonium bicarbonate and were subsequently sonicated 3 times for 30 seconds. The mixtures were centrifuged for 20 minutes, at 15,000 g, at 4°C, to remove any remaining debris. Protein samples were then mixed, in duplicates, in 1:1 ratio, to a total of 250 µg total protein each (125 µg from heavy-labeled and 125 µg from light-labeled condition). The 2 combined replicates were then denatured in a water bath for 15 minutes at 80°C, reduced with 10 mmol/L dithiothreitol (Sigma-Aldrich) for 10 minutes at 70°C, alkylated with 20 mmol/L iodoacetamide (Sigma-Aldrich) for 60 minutes and were trypsin-digested (Promega) at a ratio of 1:50 (trypsin:protein

concentration) for 8 hours. The resulting tryptic peptides were reconstituted in 120 µL of 0.26 mol/L formic acid, in 10% acetonitrile (mobile phase A).

Peptide fractionation/separation and mass spectrometry. Tryptic peptide-containing samples were subjected to strong cation exchange chromatography (SCX) using the Agilent 1100 system before LC-MS/MS, as previously described (14). Each fraction was run with a 55-minute gradient and eluted peptides were subjected to one full mass spectrometry (MS) scan (450–1450 *m/z*) in the Orbitrap at 60,000 resolution, followed by 6 data-dependent MS/MS scans in the linear ion trap (LTQ Orbitrap).

Protein identification and data analysis. Raw files from our DMSO and digitoxin-treated datasets were uploaded into MaxQuant21 version 1.1.1.25 (15) and searched with the Andromeda22 software against the nonredundant IPI. Human v.3.54 database, as previously described (16). Arg(+6) and Lys(+8) were set as heavy labeled with a maximum of 3 labeled amino acids per peptide. During the search, the IPI Human Fasta database was randomized and searched with a false-positive rate of 1% at the peptide and protein levels.

Ingenuity Pathway Analysis. Pathway analysis was done using the Ingenuity Pathway Analysis Software (Ingenuity Systems; IPA; <http://www.ingenuity.com/>; ref. 17).

Results

Characterization of the cytotoxic potency of 9 cardiac glycosides against a panel of 6 pancreatic cancer cell lines

Cardiac glycosides have been shown to induce apoptosis in tumor cells but not in primary cells such as peripheral blood mononuclear cells (PBMC) and neutrophils (3). Numerous studies have recently described potent cytotoxic and antiproliferative effects of cardiac glycosides in several cancer cell lines, including breast, prostate, melanoma, lung, leukemia, neuroblastoma and renal cancer (1). Thus, as a first step, we characterized the cytotoxic effects of nine commonly used cardiac glycosides against a panel of six pancreatic cancer cell lines. To estimate the IC₅₀ (dose that confers 50% cell death) of each drug, cells were treated in a 96-well format with ten different doses of each drug (ranging from 1 nmol/L to 1 µmol/L) and cell viability was measured by Alamar Blue 48 hours after drug exposure (Fig. 1). As illustrated, these compounds exhibited striking differences in their cytotoxic potential, despite their high structural similarities. Ranking of the cardiac glycosides in order of decreased potency is: peruvoside (23 nmol/L), bufalin (46 nmol/L), proscillaridin A (62 nmol/L), convallatoxin (66 nmol/L), digitoxin (124 nmol/L), ouabain (212 nmol/L), digoxin (344 nmol/L), digitoxigenin (645 nmol/L; values in brackets represent the mean IC₅₀ of each drug in all 6 cell lines). In all cell lines, peruvoside, proscillaridin A, bufalin, and convallatoxin appeared as

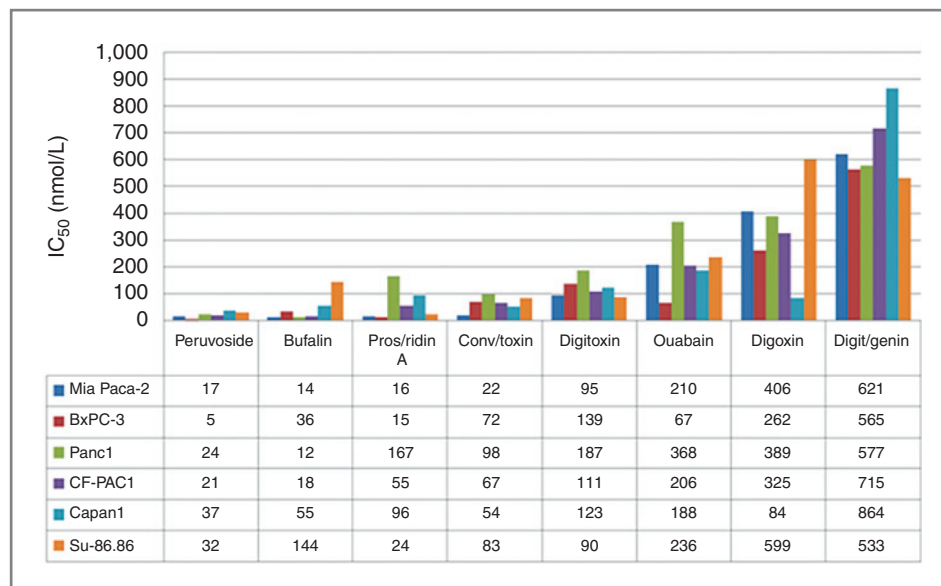


Figure 1. Evaluation of the cytotoxic potency of cardiac glycosides. Six pancreatic cancer cell lines were treated in a 96-well format with 10 different doses (8 replicates per dose) of each compound (ranging from 1 nmol/L–1 μ mol/L) and cell viability was measured by Alamar Blue 48 hours after treatment.

the most potent members of the cardiac glycoside family, followed by digitoxin, ouabain, and digoxin. In agreement with previous reports, we also identified the aglycone digitoxigenin as the least potent member of our candidates, highlighting a potentially important role of the sugar moiety for the activity of these drugs.

Characterization of cardiac glycoside-induced cell death

Next, we asked whether this reduced viability observed by Alamar Blue assays was a result of acute cell injury (necrosis) or an intracellular cell-death program (apoptosis). To test this, BxPC3, PANC-1, and MiaPaca-2 cells were treated with increasing doses of digitoxin or peruvoside (1 nmol/L to 1 μ mol/L) and lactate dehydrogenase was measured as a marker of necrosis at 6, 12, 24, and 48-hour posttreatment. Despite the fact that no necrosis was observed at doses up to 200 nmol/L with both drug treatments, even after 48 hours, Alamar Blue and 3-(4,5-Dimethylthiazol-2-yl)-2,5-diphenyltetrazolium bromide assays revealed reduced cell viability in that dose range, suggesting possible induction of programmed cell death mechanisms, instead of necrosis (data not shown). Furthermore, Annexin-V FACS analysis revealed severe (>95%) apoptosis, induced at 24 hours and 48 hours after treatment with 50 nmol/L and 100 nmol/L of both drugs (Fig. 2A). Moreover, pretreatment of cells (4 hours before drug treatment) with 200 μ mol/L of the general peptide caspase inhibitor (Z-VAD-FMK) totally rescued cells from digitoxin-induced cell death, additionally suggesting a caspase-dependent apoptotic mechanism (data not shown).

Furthermore, to gain additional time-course evidence on the cytotoxic potential of these drugs, we conducted a series of experiments to identify the time frame between cardiac glycoside treatment and induction of cell death.

BxPC-3 cancer cells were subjected to peruvoside (50 nmol/L) and digitoxin (100 nmol/L) treatment and cell viability was measured (Alamar Blue) at 16, 24, 30, 40, and 48 hours after treatment. We noticed that as early as 16-hour posttreatment, most of the cells were not alive (Supplementary Fig. S1) and therefore, we opted a more sensitive cell death assay (xCelligence assay), to capture the onset of the cardiac glycoside-induced cell death. The xCelligence system allows a real-time monitoring of cell viability upon drug addition (Fig. 1C) and we found out that in all cell lines tested (BxPC-3, Mia-PACA-2, and Panc-1) cell death phenotypes start 4-hour post-treatment with increasing doses of either peruvoside or digitoxin (Fig. 1D). These findings imply a very rapid cytotoxic effect of cardiac glycosides on the tested cancer cell lines. Furthermore, cells were treated with 8 different doses (ranging from 1 nmol/L to 1 μ mol/L) of digitoxin, digoxin, peruvoside, and gemcitabine (a very common chemotherapeutic drug for pancreatic cancer) and the built-in xCelligence software package was used to estimate the half maximum effect concentrations IC_{50} s of all 3 cardiac glycosides (and gemcitabine) against these 3 cell lines (Table 2 and Fig. 2F). Interestingly, the estimated IC_{50} values derived from the real-time monitoring xCelligence system closely correlated the IC_{50} s derived from the single-point Alamar Blue viability test.

Digitoxin activates proapoptotic pathways via the Na-K-ATPase-mediated signal transduction circuitry

The last decade, pioneering work by Xie and colleagues revealed that the Na-K-ATPase, apart from being an ion pump, is also the core member of a multiunit functional signalosome that upon cardiac steroid-binding transmits proliferative signals to the nucleus of normal cardiac myocytes. Binding of cardiac glycosides to the a-subunit

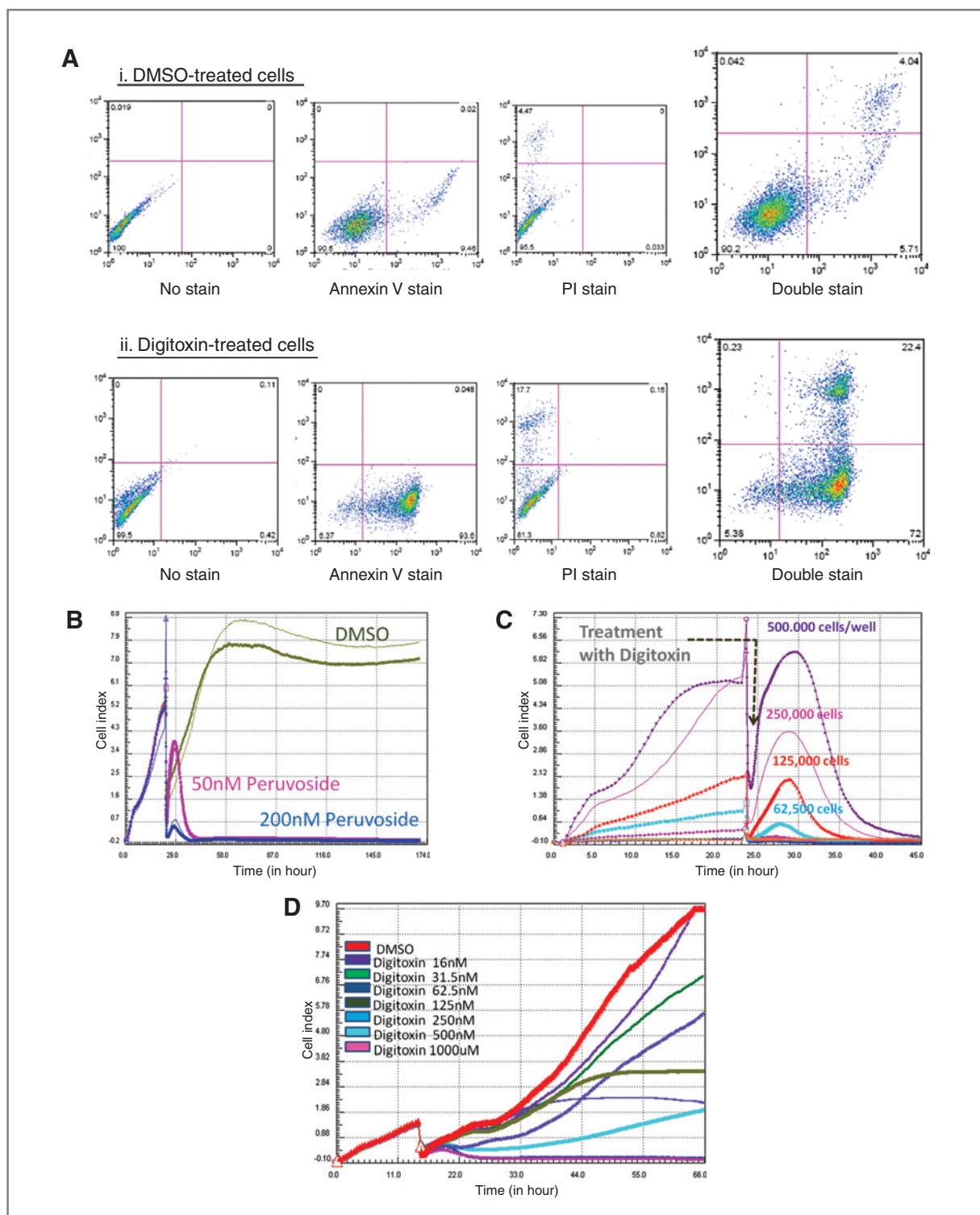


Figure 2. Characterization of cardiac glycoside-induced death. **A**, BxPC3 pancreatic cancer cells were treated with 100 nmol/L of digitoxin and apoptosis was measured with the Annexin V flow cytometric analysis. More than 90% of cells were found in either early or late apoptosis stage. Similar results were obtained after treatment of BxPC3 cells with peruvoside or bufalin (data not shown). **B**, real-time monitoring of cell viability with the xCelligence system. In the graphs, x axis corresponds to time and y axis to cell viability index. DMSO treatment did not interfere with the viability of cells (viable cell index continuously increased after DMSO treatment); however, digitoxin induced cell death in a dose–response manner (viable cell index dropped after digitoxin treatment). **C**, digitoxin-induced cell death phenotypes appeared 4 hours after treatment. Upon digitoxin treatment, cells remained attached and viable for the first 4 hours (a characteristic increase in cell index is illustrated). After that period, digitoxin induced apoptosis that lead to detachment of cells from the plate (a characteristic decrease in cell index following the 4-hour incubation with the drug). **D**, digitoxin IC_{50} determination in BxPC3 cells. Cells were treated with 8 different doses of digitoxin (ranging from 1 nmol/L–1 μ mol/L) and a cell viability index was retrieved every 5 minutes. There was a clear dose–response relationship, with the lower doses (purple, green, blue lines) conferring no cytotoxicity similar to DMSO (red line). All doses above 250 nmol/L conferred significant cytotoxicity.

of the sodium pump, allosteric activation of Src kinase, transactivation of the epidermal growth factor receptor (EGFR) and downstream activation of the Ras-dependent pathways have been shown to be important events for the transmission of the proproliferative signals in normal cardiac myocytes, smooth muscle cells, and endothelial cells (18–20).

To investigate whether the same pathways govern cardiac glycoside cytotoxic action in cancer cells, we pretreated BxPC3 cells with a chemical kinome library 12 hours before addition of a lethal IC_{90} /dose of digitoxin (500 nmol/L; Fig. 3A). In this screening, we decided to focus on digitoxin (Fig. 3B), because it is an Food and Drug Administration-approved drug and we hypothesized that preblocking of key kinases, might interfere with the efficiency of digitoxin to transmit apoptotic signals. On grounds of network redundancy (cell tries to compensate by activating alternative signaling modules), we would not expect a total rescuing effect. First, kinase inhibitors that conferred more than 30% cell death when administered alone were excluded from further investigations (5/320), because their high potency could mask a potential synergistic or antagonistic effect with digitoxin. Next, we set an arbitrary threshold at 50% cell viability and defined as potential digitoxin-associated kinases, those kinases the inhibition of which significantly reduced the cytotoxic effect of a potent dose of digitoxin (IC_{90}). The whole experiment was done in duplicate. Despite the fact that the large majority of kinase inhibitors (~75%) had none or minimal effects on digitoxin cytotoxicity, there were 14/320 kinase inhibitors identified, that significantly rescued cells from

digitoxin induced apoptosis (Fig. 3C and Supplementary Table 1). Interestingly, 12 of these 14 kinase inhibitors target kinases that are key members of the Na-K-ATPase-mediated signal transduction circuitry through which cardiac glycosides have been shown to transmit proproliferative signals to normal cells. In particular, within our hit list there were 4 different inhibitors of the Mitogen-activated protein kinase (MEK), 3 inhibitors of the EGFR, 4 inhibitors of the protein-kinase C and 1 inhibitor of the Src tyrosine kinase. Moreover, butyrolactone-I and roscovitine, 2 Cdk5 kinase inhibitors, were previously found to prevent cardiac glycoside-induced cell death in cancer cell lines (21). Our results, not only validate this finding, but also imply that additional members of the cdk family play a major role as downstream mediators of cardiac glycoside-triggered apoptosis. Overall, this is the first report to provide systematic evidence that cardiac glycosides at higher doses might induce apoptosis in cancer cells through the same pathways that induce proliferation in nontransformed cells. Increased expression of the sodium pump subunits by cancer cells might account for this differential effect of these drugs between cancer and normal cells (22–24). Further studies are necessary to fully elucidate the exact involvement of these particular kinases in the molecular mechanism of cardiac glycoside action.

Quantitative proteomic analysis (SILAC) reveals perturbation of interferon-regulated pathways in BxPC3 cells, 48 hour after treatment with a physiologically relevant dose of digitoxin

Little is known regarding global proteomic changes in cancer cells treated with cardiac glycosides. Such infor-

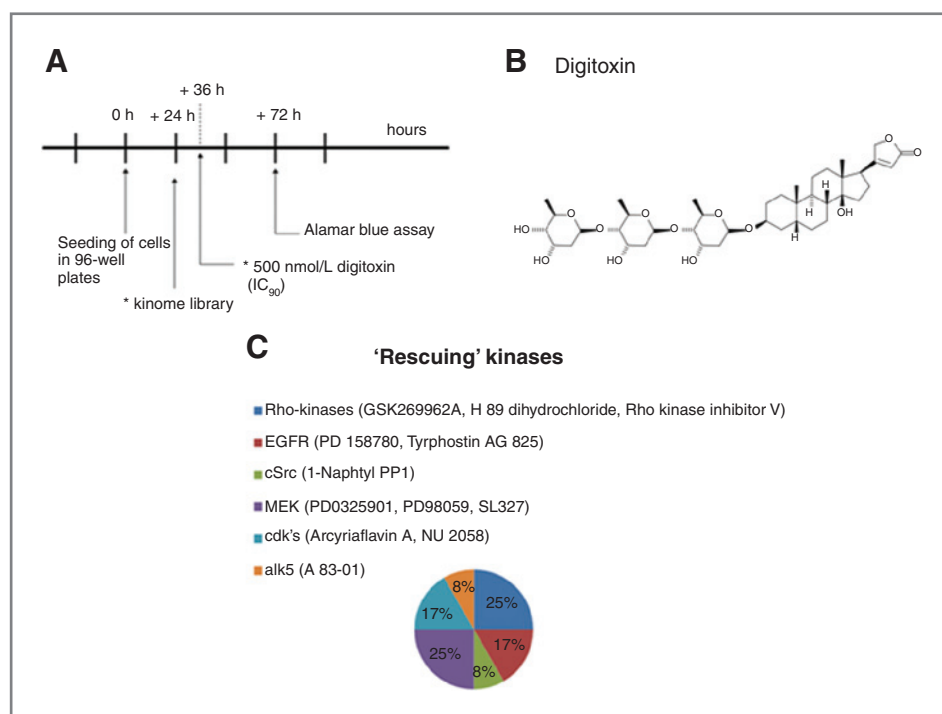
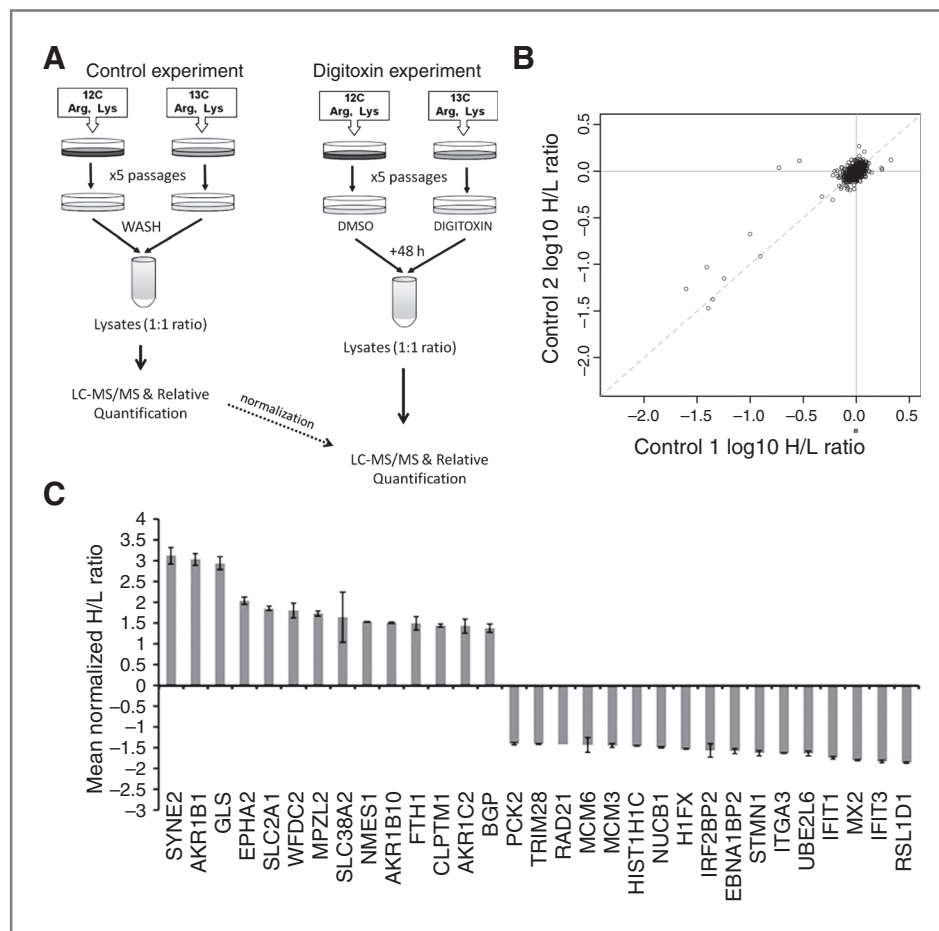


Figure 3. Digitoxin activates distinct downstream kinases. **A**, time-scale of the experiment. Kinase inhibitors were added 12 hours before digitoxin treatment and cell viability was measured 48 hours later. **B**, digitoxin structure. **C**, digitoxin activates proapoptotic pathways in cancer cells via the Na-K-ATPase-mediated signal transduction circuitry. Functional classification of rescuing kinases revealed that most hits are major kinases (cSrc, EGFR, MEK, Rho-kinases) downstream of the sodium pump's signalosome. Interestingly, cdk's also seem to play an important role in mediating apoptotic signals upon cardiac glycoside treatment.

Figure 4. Quantitative proteomic analysis of the protein perturbations induced after treatment with a physiologically relevant dose of digitoxin. **A**, graphical illustration of the SILAC procedure (metabolite labeling, sample preparation, chromatographic separation, and MS/MS-based protein identification). **B**, distribution of digitoxin-induced protein alterations. **C**, twenty-seven proteins were significantly altered upon digitoxin treatment in both replicates.



mation could provide valuable insights in responsible pathways for the observed phenotypes upon cardiac glycoside administration. In view of emerging powerful quantitative proteomic approaches, we delineated cardiac glycoside-associated proteome alterations. We used SILAC coupled to mass-spectrometry, to study large-scale proteome dynamic changes induced by a clinically relevant concentration of digitoxin (30 nmol/L) in BxPC3 pancreatic cancer cells.

Two experimental conditions (with 2 biological replicates each) were used in our study, a control group (no digitoxin) and a digitoxin-treated group. In the former, both heavy and light labeled cells were left untreated, whereas in the second group only heavy labeled cells were treated with 30 nmol/L digitoxin (light labeled cells were mock treated with DMSO; Fig. 4A). In both cases, protein samples were mixed in 1:1 heavy/light ratio (w/w) before MS analysis. Protein quantification was based on the differential intensities of the peaks of the precursor ions of heavy versus light peptides. As expected, the great majority of proteins in our control experiments were identified with a heavy/light ratio close to 1 (Supplementary Fig. S3). It should be noted

that the control experiments provided adequate normalization for the actual digitoxin group experiments by filtering out changes that were not associated to digitoxin treatment. To this extent, we were able to identify 1,932 and 2,132 proteins in the 2 digitoxin-treated biological replicates, of which 1,409 and 1,604 could be respectively quantified. The mean distribution of digitoxin-induced protein alterations is shown in Fig. 4B. In total, 27 proteins were identified whose mean expression was significantly altered ($P < 0.05$) upon digitoxin treatment in both replicates (of which 10 were upregulated and 17 were downregulated; Table 1 and Fig. 4C).

Pathway analysis

To achieve a higher-resolution molecular insight of the digitoxin-regulated proteome network in cancer cells, we analyzed the differentially expressed proteins, obtained with SILAC approach, with the Ingenuity Pathways Knowledge Software (Ingenuity Systems; IPA) and explored enrichment of canonical pathways. We identified 10 canonical pathways surpassing the statistical threshold upon treatment of cancer cells with a physiologically relevant dose of digitoxin (30 nmol/L), among which

Table 1. Proteomic alterations induced by treatment of BxPC3 cells with 30 nmol/L digitoxin

Protein names	Normalized ratio (H/L) ^a	P
Nesprin-2	3.2	<10 ⁻²⁴
Aldo-keto reductase member B1 variant	3.1	<10 ⁻³⁰
Glutaminase kidney isoform	2.8	<10 ⁻²³
Sodium-coupled neutral amino acid transporter 2	2.1	<10 ⁻⁷
Ephrin type-A receptor 2	2.0	<10 ⁻¹¹
Solute carrier family 2	1.9	<10 ⁻¹¹
Myelin protein zero-like protein 2	1.7	<10 ⁻⁷
Aldo-keto reductase family 1 member C2	1.5	<10 ⁻⁴
Normal mucosa of esophagus-specific gene 1 protein	1.5	<10 ⁻⁵
Aldo-keto reductase family 1 member B10	1.5	<10 ⁻⁵
Carcinoembryonic antigen-related cell adhesion mol 1	1.4	<10 ⁻⁴
Cleft lip and palate transmembrane protein 1	1.4	<10 ⁻⁴
Transcription intermediary factor 1-beta	0.7	<10 ⁻⁴
Double-strand-break repair protein rad21 homolog	0.7	<10 ⁻⁴
Phosphoenolpyruvate carboxykinase [GTP]	0.7	<10 ⁻⁴
Nucleobindin-1	0.7	<10 ⁻⁴
Histone H1.2	0.7	<10 ⁻⁴
Stathmin	0.7	<10 ⁻⁷
DNA replication licensing factor MCM3	0.7	<10 ⁻⁴
Ubiquitin/ISG15-conjugating enzyme E2 L6	0.7	<10 ⁻⁷
Histone H1x	0.6	<10 ⁻⁵
Integrin alpha-3	0.6	<10 ⁻⁷
Glutamine synthetase	0.6	<10 ⁻⁶
IFN-induced 56 kDa protein	0.6	<10 ⁻⁷
EBNA1-binding protein 2	0.6	<10 ⁻⁶
DNA replication licensing factor MCM6	0.6	<10 ⁻⁴
IFN-induced protein with tetratricopeptide repeats	0.6	<10 ⁻⁹
IFN-induced GTP-binding protein Mx2	0.6	<10 ⁻⁹
DNA replication licensing factor MCM5	0.6	<10 ⁻⁹
IFN regulatory factor 2-binding protein 2	0.5	<10 ⁻⁶
Ribosomal L1 domain-containing protein 1	0.5	<10 ⁻¹⁰

^aValues are means of 2 biological replicates.

granzyme A and interferon (IFN) signaling, were the top ones (Fig. 5A). Interestingly, these 2 pathways were followed by certain metabolism-related pathways, such as glutamate, nitrogen, D-glutamine, D-glutamate, and pyruvate metabolism, further denoting that cardiac glycosides could disturb major metabolic and energy-producing processes. Our findings add further support to the recent hypothesis that digitoxin selectively targets

cancer cells through inhibition of glycolysis (5). We further organized the cardiac glycoside-regulated proteome into distinct interaction networks, through the IPA software, to predict how digitoxin treatment might influence the crosstalk among proteins that interact with each other. We identified one major network (Fig. 5B) in which IFN-alpha (IFN- α) and IFN-beta (IFN- β), as well as other members of the IFN-family were found to nucleate clusters of protein interactions. These proteins may act as organizational hubs, proteins that regulate multiple protein-protein interactions and networks downstream of digitoxin action. Conclusively, pathway analysis (canonical enrichment and network analysis) depicted interferon signaling as a potent mediator of cellular changes upon cg treatment; this observation is in concordance with the very recent findings, showing that cardiac glycosides are potent inhibitors of IFN- β gene expression, implicating potential benefits for the use of these drugs for the treatment of inflammatory and auto-

Table 2. Digitoxin IC₅₀ determination in BxPC3 cells

IC ₅₀ (nmol/L)	BxPC-3	Mia-Paca-2	Panc-1
Digitoxin	131	122	197
Digoxin	260	290	320
Peruvoside	16	25	72
Gemcitabine	NA	NA	NA

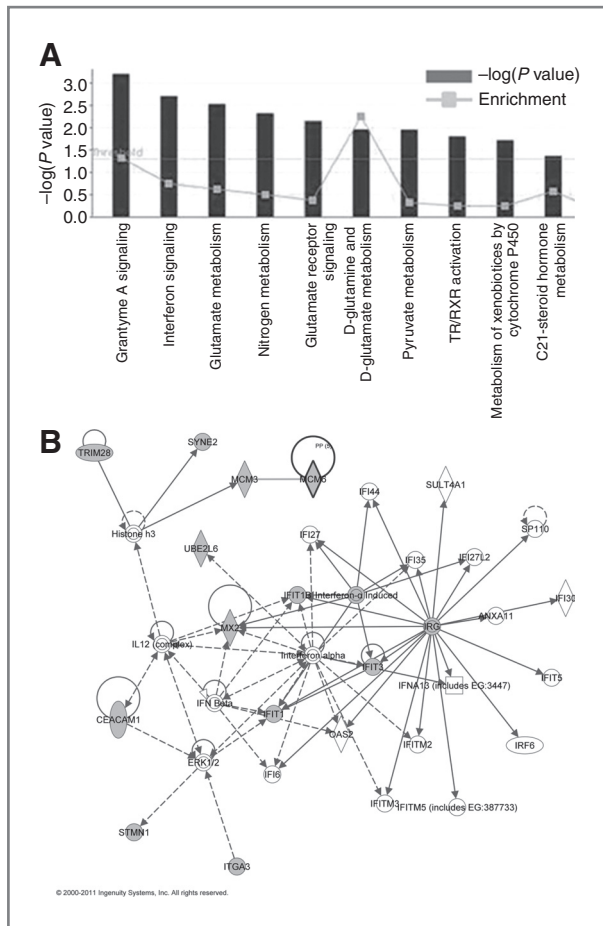


Figure 5. Ingenuity pathway analysis. A, the top 10 canonical pathways identified as significantly altered upon digitoxin treatment. B, IFN-signaling networks appeared as the major signaling hubs downstream of digitoxin action.

immune diseases in which IFN or TNF are hyperactivated (25).

Discussion

Cardiac glycosides represent a class of naturally derived compounds that have been in clinical use for centuries. Members of this family (digoxin, digitoxin) have been used for the treatment of heart failure and atrial arrhythmia, and the mechanism of their positive inotropic effects is well characterized (1). Epidemiologic studies describing improved outcomes of breast cancer patients receiving cardiac glycosides and a lower risk for leukemia, kidney, and urinary tract cancer, triggered new interest in the therapeutic roles of these compounds against neoplastic diseases (26).

In vitro studies have shown that cardiac glycosides, at low doses, can preferentially induce cell death to cancer cells, compared with their nonmalignant counterparts. Recent findings that cancer biopsies express much higher levels of different sodium pump subunits might provide

a rational basis for this increased sensitivity of cancer cells to the effects of these drugs. Several mechanisms have been proposed by us and others, to account for their cytotoxic action, including inhibition of HIF-1 synthesis (27), downregulation of c-MYC (28), inhibition of topoisomerase II (29), upregulation of death receptors DR4 and DR5 (30), increased expression of ROS (31), alterations in membrane fluidity (32) and anoikis induction (33). Moreover, Wang and colleagues, recently showed that digoxin and other cardiac glycosides inhibit p53 synthesis by a mechanism relieved by Sarcoma kinase (Src kinase) or mitogen-activated protein kinase (MAPK) inhibition, highlighting a potential benefit for the use of these drugs in human cancers with a gain of function p53 mutation (34).

In this report, we showed that cardiac glycosides induce caspase-dependent apoptosis in a panel of cancer cell lines *in vitro*. Of clinical importance would be the understanding of why different cell lines respond differently to these drugs. It has been recently proposed, that the differential sensitivities of cancer cells to cardiac glycosides might be explained by their intrinsic differences in the relative expression of sodium pump subunits. Indeed, the relative $\alpha 3/\alpha 1$ sodium pump subunit expression has been shown to correlate with the sensitivity of each cell line to the cytotoxic effects of these drugs (35). Future establishment of clear correlations between different $\text{Na}^+\text{-K}^+\text{-ATPase}$ isoform expression patterns and their sensitivities to cardiac glycosides might provide a more targeted direction to the potential anti-cancer effects of these compounds.

It is now well shown that the sodium pump, apart from its established role in regulating ion homeostasis, is a versatile signal transducer that acts as a scaffold molecule for the formation of a multicore signalosome complex located in the caveolae of most cells (36). Binding of cardiac steroids to the sodium pump and concomitant activation of that signalosome activates multiple downstream signaling pathways leading to either apoptosis or cell growth, in a cell type-specific manner. To investigate, in a nonbiased way, the kinases that are important for the cytotoxic action of cardiac steroids in cancer cells, we used a targeted functional screening approach and our identified candidates constitute established members of that signalosome (EGFR, Src, MEK1 and MEK2, and Rho-kinases). Although the mechanism is not fully elucidated, our findings are in concordance with the notion that activation of Src and MAPK signaling pathways are the main mediators of the cytotoxic action of cardiac glycosides.

Despite the great phenotypic success of cardiac glycosides in mouse models of cancer progression (that paved the way for entrance of these compounds to clinical trials), the extent to which these findings could be translated to humans is rather questionable (37, 38). Mice are inherently much more tolerant to the cardiotoxic effects of cardiac glycosides and therefore they represent a poor

toxicity model for the study of cardiac glycosides. Indeed, the alpha chain of the murine sodium pump is approximately 1,000 times less sensitive for cardiac glycosides than its human orthologue and therefore, rodents can tolerate much higher levels of cardiac glycosides compared with humans (39). This is the first study in which the effects of a physiologically relevant (and nontoxic) dose of digitoxin in pancreatic cancer cells were analyzed with quantitative proteomics. We identified that at physiologic doses, cardiac glycosides cause a significant downregulation of the expression of many interferon-induced proteins, a finding which coincides with a recent study of the Maniatis group in which cardiac glycosides were identified as potent inhibitors of IFN- β gene expression and implicated a potential therapeutic use of these drugs for the treatment of IFN-related diseases, such as the autoimmune disease systemic lupus erythematosus. In parallel, a significant upregulation of many members of the aldo-keto reductase (AKR) family was noticed. Among others, AKR proteins (e.g., AKR1B10) are well-established antioxidant and cytoprotective proteins. A possible scenario could be that digitoxin-induced ROS production and concomitant redox cell stress might result in the upregulation of these proteins, in which case AKRs might represent another good target for combination therapy with digitoxin. Finally, the increase in the expression of sodium-regulated proteins (sodium-coupled

neutral amino acid transporter 2), could be the direct result of the intracellular increase of Na⁺ concentration following blockage of the sodium pump by cardiac glycosides.

Overall, this study shows a proteomic and kinome-based snapshot of molecular events downstream of digitoxin action in pancreatic cancer cells. This high-throughput approach has validated and brought together promising candidate pathways and key signaling molecules associated with digitoxin action. Most importantly, novel key molecules have been identified (e.g., IFN and IFN-regulated pathways) that might help us understand further the emerging pleiotropic mechanism of these drugs.

Disclosure of Potential Conflict of Interest

No potential conflicts of interest were disclosed.

Acknowledgments

We thank the Ontario Institute for Cancer Research (OICR), Medicinal Chemistry Platform for providing the kinome library to us.

The costs of publication of this article were defrayed in part by the payment of page charges. This article must therefore be hereby marked *advertisement* in accordance with 18 U.S.C. Section 1734 solely to indicate this fact.

Received June 9, 2011; revised July 27, 2011; accepted July 30, 2011; published OnlineFirst August 22, 2011.

References

- Prassas I, Diamandis EP. Novel therapeutic applications of cardiac glycosides. *Nat Rev Drug Discov* 2008;7:926-35.
- Stenkvist B, Bengtsson E, Eriksson O, Holmquist J, Nordin B, Westman-Naeser S. Cardiac glycosides and breast cancer. *Lancet* 1979;1:563.
- Sreenivasan Y, Raghavendra PB, Manna SK. Oleandrins-mediated expression of Fas potentiates apoptosis in tumor cells. *J Clin Immunol* 2006;26:308-22.
- Khan MI, Chesney JA, Laber DA, Miller DM. Digitalis, a targeted therapy for cancer? *Am J Med Sci* 2009;337:355-9.
- Lopez-Lazaro M. Digitoxin as an anticancer agent with selectivity for cancer cells: possible mechanisms involved. *Expert Opin Ther Targets* 2007;11:1043-53.
- Beheshti ZR, Lau KS, Hurren R, Datti A, Ashline DJ, Gronda M, et al. Inhibition of the sodium/potassium ATPase impairs N-glycan expression and function. *Cancer Res* 2008;68:6688-97.
- Mijatovic T, Van Quaquebeke E, Delest B, Debeir O, Darro F, Kiss R. Cardiotonic steroids on the road to anti-cancer therapy. *Biochim Biophys Acta* 2007;1776:32-57.
- Vaklavas C, Chatzizisis YS, Tsimberidou AM. Common cardiovascular medications in cancer therapeutics. *Pharmacol Ther* 2011;130:177-90.
- Prassas I, Paliouras M, Datti A, Diamandis EP. High-throughput screening identifies cardiac glycosides as potent inhibitors of human tissue kallikrein expression: implications for cancer therapies. *Clin Cancer Res* 2008;14:5778-84.
- Urcan E, Haertel U, Styllou M, Hickel R, Scherthan H, Reichl FX. Real-time xCELLigence impedance analysis of the cytotoxicity of dental composite components on human gingival fibroblasts. *Dent Mater* 2010;26:51-8.
- Hanusova V, Kralova V, Schroterova L, Trilecova L, Pakostova A, Skalova L. The effectiveness of oracin in enhancing the cytotoxicity of doxorubicin through the inhibition of doxorubicin deactivation in breast cancer MCF7 cells. *Xenobiotica* 2010;40:681-90.
- Coma I, Herranz J, Martin J. Statistics and decision making in high-throughput screening. *Methods Mol Biol* 2009;565:69-106.
- Ong SE, Blagoev B, Kratchmarova I, Kristensen DB, Steen H, Pandey A, Mann M. Stable isotope labeling by amino acids in cell culture, SILAC, as a simple and accurate approach to expression proteomics. *Mol Cell Proteomics* 2002;1:376-86.
- Batruch I, Lecker I, Kagedan D, Smith CR, Mullen BJ, Grober E, Lo KC, Diamandis EP, Jarvi KA. Proteomic analysis of seminal plasma from normal volunteers and post-vasectomy patients identifies over 2000 proteins and candidate biomarkers of the urogenital system. *J Proteome Res* 2011;10:941-53.
- Cox J, Mann M. MaxQuant enables high peptide identification rates, individualized p.p.b.-range mass accuracies and proteome-wide protein quantification. *Nat Biotechnol* 2008;26:1367-72.
- Cox J, Neuhauser N, Michalski A, Scheltema RA, Olsen JV, Mann M. Andromeda: A Peptide Search Engine Integrated into the MaxQuant Environment. *J Proteome Res* 2011;10:1794-805.
- Available from: <http://www.ingenuity.com>.
- Haas M, Wang H, Tian J, Xie Z. Src-mediated inter-receptor cross-talk between the Na⁺/K⁺-ATPase and the epidermal growth factor receptor relays the signal from ouabain to mitogen-activated protein kinases. *J Biol Chem* 2002;277:18694-702.
- Wang H, Haas M, Liang M, Cai T, Tian J, Li S, Xie Z. Ouabain assembles signaling cascades through the caveolar Na⁺/K⁺-ATPase. *J Biol Chem* 2004;279:17250-9.
- Pierre SV, Xie Z. The Na, K-ATPase receptor complex: its organization and membership. *Cell Biochem Biophys* 2006;46:303-16.
- Lin H, Juang JL, Wang PS. Involvement of Cdk5/p25 in digoxin-triggered prostate cancer cell apoptosis. *J Biol Chem* 2004;279:29302-7.

22. Sakai H, Suzuki T, Maeda M, Takahashi Y, Horikawa N, Minamimura T, et al. Up-regulation of Na(+),K(+)-ATPase alpha 3-isoform and down-regulation of the alpha1-isoform in human colorectal cancer. *FEBS Lett* 2004;563:151-4.
23. Shibuya K, Fukuoka J, Fujii T, Shimoda E, Shimizu T, Sakai H, Tsukada K. Increase in ouabain-sensitive K+-ATPase activity in hepatocellular carcinoma by overexpression of Na+, K+-ATPase alpha 3-isoform. *Eur J Pharmacol* 2010;638:42-6.
24. Mijatovic T, Jungwirth U, Heffeter P, Hoda MA, Dornetshuber R, Kiss R, Berger W. The Na+/K+-ATPase is the Achilles heel of multi-drug-resistant cancer cells. *Cancer Lett* 2009;282:30-4.
25. Ye J, Chen S, Maniatis T. Cardiac glycosides are potent inhibitors of interferon-beta gene expression. *Nat Chem Biol* 2011;7:25-33.
26. Newman RA, Yang P, Pawlus AD, Block KI. Cardiac glycosides as novel cancer therapeutic agents. *Mol Interv* 2008;8:36-49.
27. Zhang H, Qian DZ, Tan YS, Lee K, Gao P, Ren YR, et al. Digoxin and other cardiac glycosides inhibit HIF-1alpha synthesis and block tumor growth. *Proc Natl Acad Sci U S A* 2008;105:19579-86.
28. Mijatovic T, De Neve N, Gailly P, Mathieu V, Haibe-Kains B, Bontempi G, et al. Nucleolus and c-Myc: potential targets of cardenolide-mediated antitumor activity. *Mol Cancer Ther* 2008;7:1285-96.
29. Hashimoto S, Jing Y, Kawazoe N, Masuda Y, Nakajo S, Yoshida T, et al. Bufalin reduces the level of topoisomerase II in human leukemia cells and affects the cytotoxicity of anticancer drugs. *Leuk Res* 1997;21:875-83.
30. Frese S, Frese-Schaper M, Andres AC, Miescher D, Zumkehr B, Schmid RA. Cardiac glycosides initiate Apo2L/TRAIL-induced apoptosis in non-small cell lung cancer cells by up-regulation of death receptors 4 and 5. *Cancer Res* 2006;66:5867-74.
31. Xie Z. Molecular mechanisms of Na/K-ATPase-mediated signal transduction. *Ann N Y Acad Sci* 2003;986:497-503.
32. Manna SK, Sreenivasan Y, Sarkar A. Cardiac glycoside inhibits IL-8-induced biological responses by downregulating IL-8 receptors through altering membrane fluidity. *J Cell Physiol* 2006;207:195-207.
33. Simpson CD, Mawji IA, Anyiwe K, Williams MA, Wang X, Venugopal AL, et al. Inhibition of the sodium potassium adenosine triphosphatase pump sensitizes cancer cells to anoikis and prevents distant tumor formation. *Cancer Res* 2009;69:2739-47.
34. Wang Z, Zheng M, Li Z, Li R, Jia L, Xiong X, et al. Cardiac glycosides inhibit p53 synthesis by a mechanism relieved by Src or MAPK inhibition. *Cancer Res* 2009;69:6556-64.
35. Lin Y, Ho DH, Newman RA. Human tumor cell sensitivity to oleandrin is dependent on relative expression of Na+, K+ -ATPase subunitst. *J Exp Ther Oncol* 2010;8:271-86.
36. Xie Z, Xie J. The Na/K-ATPase-mediated signal transduction as a target for new drug development. *Front Biosci* 2005;10:3100-9.
37. Lopez-Lazaro M. Digoxin, HIF-1, and cancer. *Proc Natl Acad Sci U S A* 2009;106:E26.
38. Perne A, Muellner MK, Steinrueck M, Craig-Mueller N, Mayerhofer J, Schwarzingler I, et al. Cardiac glycosides induce cell death in human cells by inhibiting general protein synthesis. *PLoS One* 2009;4:e8292.
39. Lin Y, Dubinsky WP, Ho DH, Felix E, Newman RA. Determinants of human and mouse melanoma cell sensitivities to oleandrin. *J Exp Ther Oncol* 2008;7:195-205.